Available online at www.sciencedirect.com
ScienceDirect
Advances in Space Research 39 (2007) 1767–1772
ADVANCES IN SPACE RESEARCH (a COSPAR publication)
www.elsevier.com/locate/asr

The speed of halo Coronal Mass Ejections and properties of associated active regions ☆

Yang Liu

W.W. Hansen Experimental Physics Laboratory, Stanford University, Stanford, CA 94305-4085, United States

Received 9 November 2006; received in revised form 6 March 2007; accepted 16 March 2007

Abstract

In this study, we looked for any correlations between speed of active region-related halo Coronal Mass Ejections (CMEs) and the energy contained in active regions. Twenty one CMEs from the Coordinated Data Analysis Workshops (CDAW) event list are chosen to carry out this research. The solar sources of the CMEs have been carefully determined by the CDAW source identification team using various methods. This study shows that (1) there is no correlation between potential energy of active regions and the associated CMEs' speed; (2) there is no correlation between net magnetic flux of active regions and the associated CMEs' speed. Net magnetic flux of an active region is defined here as sum of the positive and negative magnetic fluxes of this active region, and may thus represent the large-scale magnetic flux that connects this active region and the remote areas. Based on a limited sample of eight events that could be adequately modeled for analysis of free energy of the active regions, this study further shows that there is a correlation between free energy density of active regions and speed of the associated CMEs.

Keywords: Solar active regions; Magnetic energy; Halo Coronal Mass Ejections

1. Introduction

On significantly different spatial scales, flares and Coronal Mass Ejections (CMEs) are two major manifestations displaying eruptive release of energy. Flares usually occur within active regions, showing disturbances within localized areas. It is thus considered that flares are related to smaller-scale magnetic fields. CMEs, on the other hand, are generally believed to be large scale or even global phenomena, related to the large-scale magnetic field. Although there is still uncertainty about the relationship between flares and CMEs, observations give increasing evidence that at least the timing of some CMEs are highly associated with flares (e.g. Zhang et al., 2001). Recent studies further demonstrate correlation between soft X-ray flux of the flares and speeds of the associated CMEs (Moon et al., 2002; Zhang et al., 2004), and correlation between CMEs' acceleration and magnetic reconnection flux, inferred by separation of the two bright ribbons of the associated flares (Qiu et al., 2004; Qiu and Yurchyshyn, 2005; Jing et al., 2005). As it is generally believed that the energy released during flares and CMEs is primarily the free energy stored in the magnetic field in the corona, it is reasonable to search for relationship between magnetic energy of active regions and speed of their associated CMEs. This is the purpose of this research.

The paper is organized as follows. In Section 2, we describe how to estimate magnetic energy of an active region. We present a sample of halo CMEs and our calculation in Section 3. The results are presented in Section 4. In Section 5, we conclude this study.

☆ The author wishes to thank the anonymous referees for comments and suggestions that help improve the manuscript. The CDAW source identification team is appreciated for their effort on determining the solar sources of the halo CMEs that provides basic dataset for this research. The team includes E. Cliver, N. Gopalswamy, J. Kapser, N. Nitta, I. Richardson, B. Thompson, D. Webb, C. Wu, S. Yashiro, J. Zhang, A. Zhukov, etc. SOHO is a project of international cooperation between ESA and NASA.

E-mail address: yliu@quake.stanford.edu.

0273-1177/$30
doi:10.1016/j.asr.2007.03.043

2. Estimate of energy of solar active regions

In this research, we will examine three quantities that may represent magnetic energy in active regions: potential energy, free energy density and magnetic helicity density. To compute potential energy in an active region, we first extrapolate potential field from MDI magnetograms using a Green Function method proposed by Chiu and Hilton (1977). Then, we calculate the energy from the computed field. For each active region, the energy is estimated in a cube of $300 \times 300 \times 300\ \text{arcsec}^3$. We believe this cube roughly contains the entire active region.

We use a simple model to estimate free energy of solar active regions. We assume that an active region only has one single flux tube. The free energy of this flux tube can be expressed as,

$$E = \frac{1}{2} L I^2, \qquad (1)$$

where L is inductance that is proportional to the length of the tube (Melrose, 1995), and I is electric current. The energy density that we are going to calculate here is E/l, where l is the length of the tube.

We compute I by assuming the flux tube is force free. The force free field α is determined by comparing the soft X-ray bright loops and the calculated linear force free field lines. First, we choose the bright loops that actually erupt during that flare. They are thus deemed to be involved in the event. Then, we compare the bright loops with the linear force free fields computed from different α. The α we finally choose gives a linear force free field that best fits the loops. Shown in Fig. 1 is an example illustrating how we select an α. The left panels exhibit soft X-ray bright loops before (top) and after (bottom) an eruptive event that occurred on May 12, 1997. The bright loops change from a sigmoidal structure to the post-eruptive arcades. A movie from soft-X ray data clearly shows that this sigmoidal

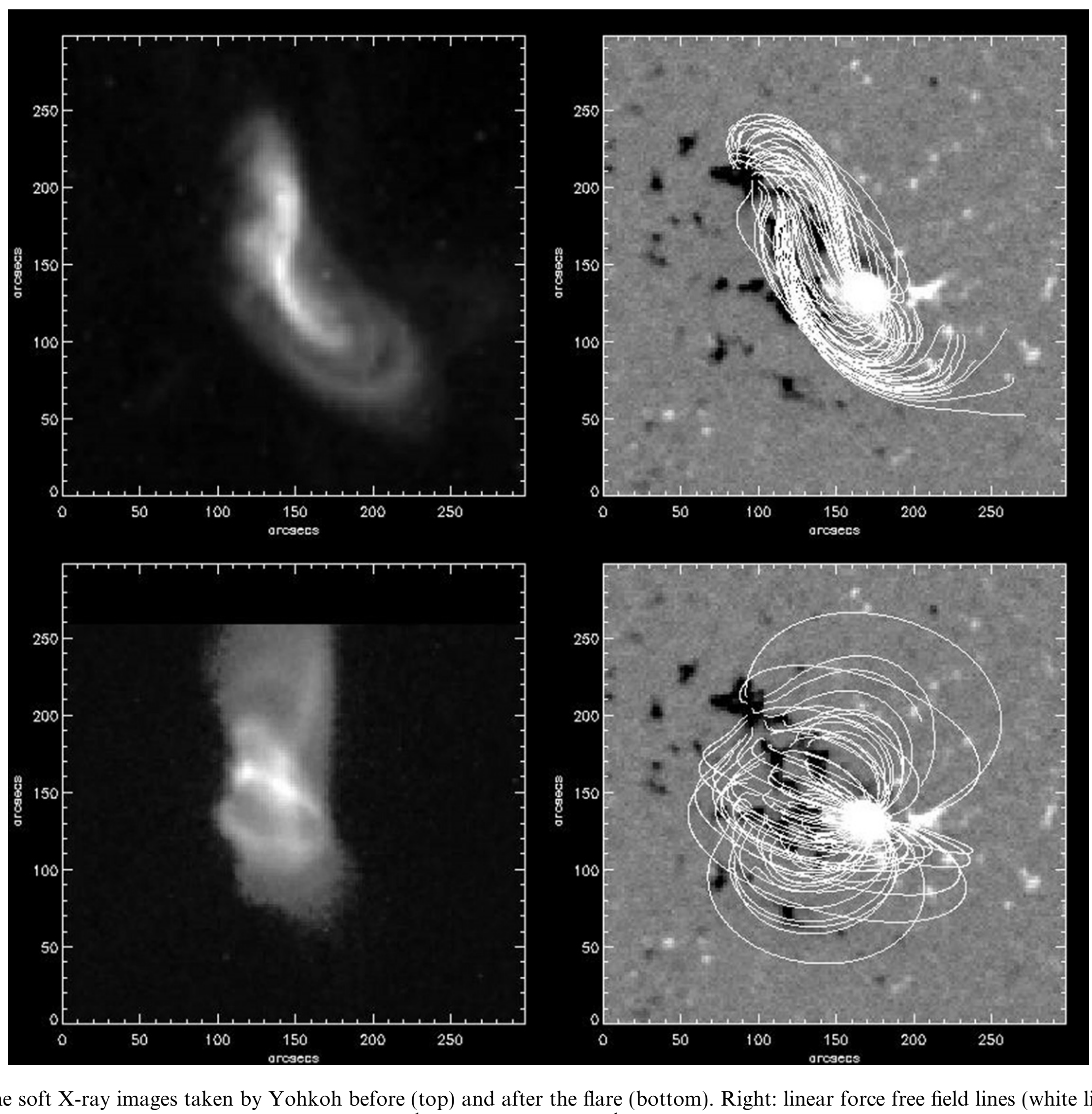

Fig. 1. Left: the soft X-ray images taken by Yohkoh before (top) and after the flare (bottom). Right: linear force free field lines (white lines) from MDI magnetograms. The α for these calculations are $-0.02\ \text{arcsec}^{-1}$ (top) and $0.0\ \text{arcsec}^{-1}$ (bottom), respectively. Only the field lines that match the bright loop structures are shown here.

structure erupted during the event, suggesting that this structure is actually involved in this eruption. This event was studied from various perspectives in the past (Plunkett et al., 1998; Thompson et al., 1998; Webb et al., 2000; Liu, 2004). In the right panels are the linear force free field lines computed from MDI magnetograms. The α chosen here is -0.02 arcsec^{-1} (top) and 0.0 (bottom), respectively. It is seen that the calculated field lines match the bright loop structures pretty well. Thus an α of -0.02 arcsec^{-1} is chosen for the erupted flux tube in this active region (AR8038). As a comparison, we also calculate an average α of this active region from vector magnetic field data taken before the event at National Astronomical Observatory of Japan. It is -0.01 arcsec^{-1}. Using this value, we also compute linear force free field (see Fig. 2). The field lines do not match the erupted loops as well as that from an α of -0.02 arcsec^{-1}.

We also estimate magnetic helicity of the active regions because it is related to free energy (e.g. Georgoulis and LaBonte, submitted for publication). For a single, isolated and closed magnetic tube, the magnetic helicity, H, can be expressed as,

$$H = (T + W)\Phi^2, \quad (2)$$

where T is the overall twist number, W is the overall writhe number (e.g. Moffatt and Ricca, 1992; Berger, 1999), and Φ is magnetic flux of the tube. The magnetic helicity density is defined here as H/l, where l is the length of the tube. T and W can be roughly estimated using force free α and tilt angle of the active region (e.g. Tian and Liu, 2003). The tilt angle of an active region is defined as the angle formed by the equator and the line connecting the locations of the leading and following magnetic fields of the active region (Howard, 1991). The locations are the magnetic flux-weighted positions of the opposite polarity magnetic fields of the active region (Howard, 1989). The force free α of an active region is determined by comparing bright loops in the Yohkoh soft X-ray images and the calculated linear force free field lines, as described above.

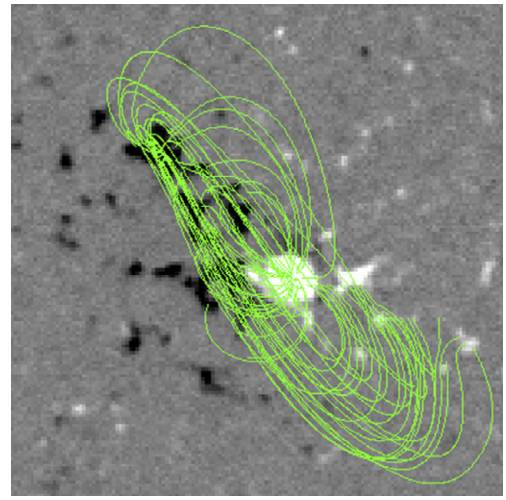

Fig. 2. Linear force free field lines (green lines) from a MDI magnetogram. The α chosen here for this calculation is -0.01 arcsec^{-1}, the average of α computed from a set of vector magnetic field data taken before the flare at National Astronomical Observatory of Japan. (For interpretation of the references to colour in this figure legend, the reader is referred to the web version of this article.)

3. Data

The events studied in this research are chosen from the Coordinate Data Analysis Workshop (CDAW) event list

Table 1
The halo CMEs and their associated active regions

ID	Time yy/mm/dd UT	Speed (km/s)	AR	PE[a] (in e32 ergs)	Tilt (degree)	α (arcsec^{-1})	Net flux (Mx)	Distance (in e7 m)
03	97/05/12 0530	464	8038	0.374	22.4	−0.020	−6.43e18	5.38
05	97/11/04 0448	785	8100	5.468	26.3	0.015	−2.82e21	6.18
09	98/05/02 1406	938	8210	4.434	−154.0		−3.13e21	2.19
17	98/11/05 2044	1119	8375	4.774	26.5	0.015	1.66e21	5.17
27	00/07/14 1054	1674	9077	5.234	−71.4		−5.29e21	2.62
29	00/08/09 1630	702	9114	3.900	10.6	−0.01	3.01e21	6.17
32	00/10/09 2350	798	9182	1.321	169.0		6.34e21	3.21
37	01/03/29 1026	942	9393	17.93	−15.8		1.54e22	1.94
42	01/09/24 1030	2402	9632	4.953	−25.0	0.025	2.19e21	2.51
44	01/09/29 1154	509	9636	3.431	−21.4	0.020	2.45e21	7.07
46	01/10/25 1526	1092	9672	5.318	−155.0		5.32e21	3.78
47	01/11/04 1635	1810	9684	5.087	−18.1	−0.015	−3.32e20	5.65
48	01/11/22 2330	1437	9704	3.487	−160.0	0.02	−1.12e22	5.71
50	02/04/15 0350	720	9906	7.402	−11.6		−5.62e21	6.28
51	02/04/17 0826	1240	9906	6.097	−8.90		−4.00e21	5.06
52	02/05/08 1350	614	9934	3.929	−22.7		−4.59e21	4.52
54	02/07/29 1207	562	0039	11.43	−8.56		−5.41e21	1.54
68	03/10/28 1130	2459	0486	18.71	24.6		1.38e21	1.60
69	03/10/29 2054	2029	0486	21.25	35.1		−2.23e21	2.17
70	03/11/18 0850	1660	0501	3.432	28.2		−6.98e21	1.37
76	04/07/25 1454	1333	0652	13.81	4.80		9.81e20	6.38

[a] PE stands potential energy.

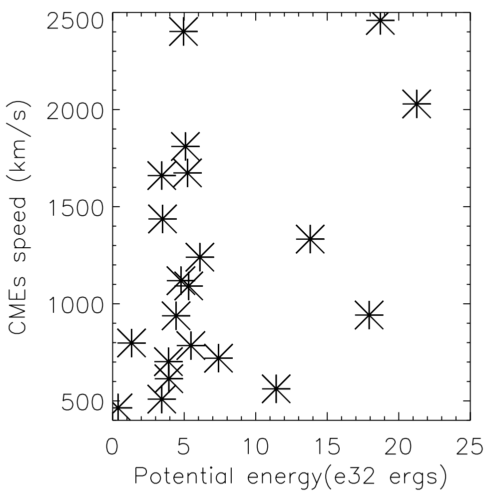

Fig. 3. Speed of the halo CMEs versus potential energy of the associated active regions. The potential energy in a cube of $300 \times 300 \times 300$ arcsec^3 is estimated for an active region.

available on line at http://cdaw.gsfc.nasa.gov/geomag_cdaw/ based on two criteria: (1) the event is a halo CME; and (2) its solar source is associated with an active region. Identifying the solar source of a halo CME is done independently by several groups including J. Zhang, S. Yashiro and N. Gopalswamy, H. Cane and I. Richardson, and D. Webb. The selected events are listed in Table 1. The first column of this table is the CDAW event identification number. The occurrence time and speed of a CME are listed in the second and third columns. The speed of a CME is computed by measuring the heights of the leading edge of the CME shown in LASCO C2 and C3 observations. Here we take the average speed from the list that is derived by fitting the height–time plot using a first-order polynomial (see Yashiro et al., 2004 for more details). Thus it is the speed in the plane of sky. The NOAA number of the associated active region is in the fourth column. Following the active region number are potential energy, tilt angle, force free field α, and the net magnetic flux of this active region. The distance between the magnetic flux-weighted positions of opposite polarity magnetic fields of the active region is in the last column. In this study, we only use the erupted bright loops shown in Yohkoh soft X-ray images to determine the force free α. Only eight events can be modeled for analysis of free energy of the active regions. For the remaining 13 events, either there was no Yohkoh X-ray data available or the calculated linear force-free field lines cannot be fitted to the X-ray loops.

4. Results

Shown in Fig. 3 is a scatter plot between CMEs' speed and potential energy of the active regions. No correlations can be seen. We also examine another two parameters, the distance of flux-weighted positions of opposite polarity magnetic fields of an active region and the net magnetic flux (see Fig. 4). The reasons to examine these parameters are (1) such a distance is found to be somehow related to flare and CME productivity of an active region (Guo et al., 2006), and (2) the net magnetic flux of an active region might be related to CMEs because it may represent the large-scale flux that connects this active region and remote areas. For this consideration, we only plot in Fig. 4 the values of net flux without sign. From this figure, however, we do not find any correlations.

A correlation between speed of the halo CMEs and free energy density of the associated active regions is shown in Fig. 5. The linear Pearson correlation coefficient is computed to be 0.61 for the eight pairs of data, suggesting that a correlation between them is significant at a level of greater than 80%. This suggests that kinematic energy of a halo CME is contributed dominantly from free energy of the associated active region. This further implies an underlying link between localized active regions and the global manifestation of CMEs, as has been suggested by many others (e.g. Zhang et al., 2001, and reference therein). As magnetic helicity is related to free energy, it is not

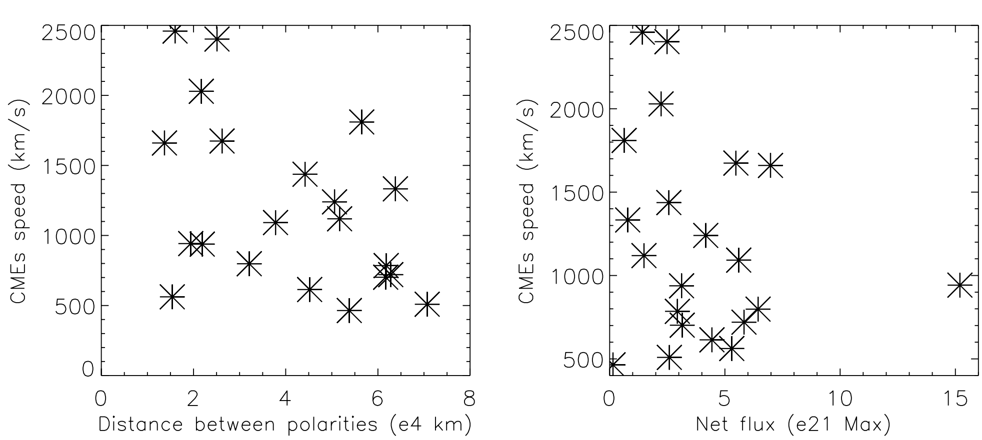

Fig. 4. Left: CMEs speeds versus distances of flux-weighted positions of opposite polarity magnetic fields of active regions. Right: CMEs' speed versus net magnetic flux (without sign) in the active regions.

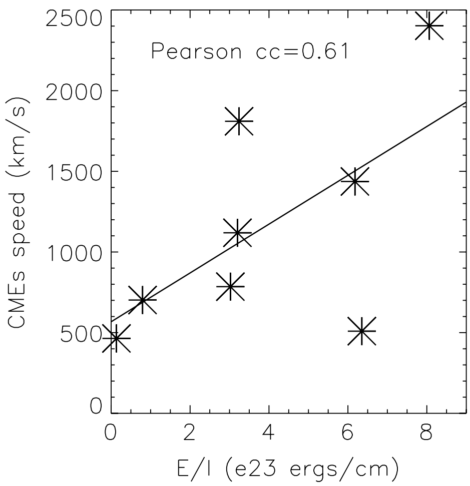

Fig. 5. A scatter plot of CMEs speeds and free energy density of active regions. The free energy density of an active region is defined as *E*/*l*, the free energy per length, where *E* is the free energy of the erupted magnetic tube in this active region that is computed from Eq.(1), and *l* is the length of the tube. The correlation coefficient is 0.61. The solid line shows the least-squares linear fit to the data points.

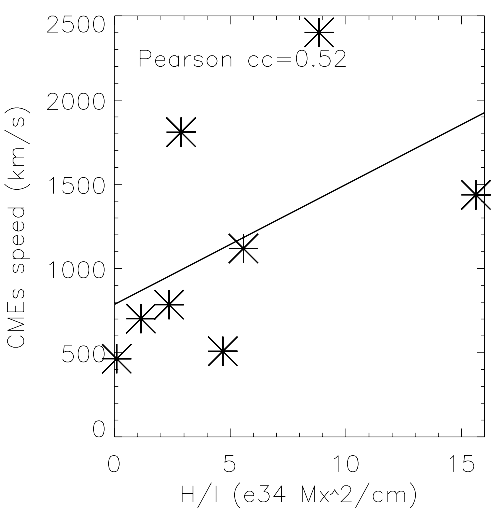

Fig. 6. CMEs speeds versus magnetic helicity density of the active regions. The helicity density of an active region is defined as *H*/*l*, the helicity per length, where *H* is magnetic helicity of the erupted magnetic tube in this active that is computed from Eq. (2), and *l* is the length of the tube. The linear Pearson correlation coefficient is computed to be 0.52. The solid line represents the least-squares linear fit to the data.

surprising to see a correlation between speed of the halo CMEs and helicity density of the active regions (see Fig. 6). The linear Pearson correlation coefficient is 0.52, yielding a correlation at a significant level of 80%.

5. Conclusions

In this research, we look for any correlations between speed of the halo CMEs and energy of the associated active regions. We have analyzed 21 halo CMEs selected from the CDAW event list. No correlations are found between the CMEs' speed and the potential energy of the associated active regions. We did not see any correlations between CMEs' speed and the distance of flux-weighted positions of opposite polarity magnetic fields of active regions that is suggested to be a measure for flare and CME productivity of an active region. We did not see any correlations between CMEs' speed and net magnetic flux of the active regions either, although the net flux of an active region might be related to CMEs because it probably connects this active region and remote areas. For 8 of these 21 halo CMEs, we are able to calculate the linear force free field lines that match the shapes of the erupted soft X-ray loops. With a simple model, we estimate free energy density and helicity density in the active regions. We found correlations between CMEs' speed and free energy density and between CMEs' speed and helicity density. This implies that the kinematic energy of a halo CME is contributed dominantly from free energy of the associated active region.

References

Berger, M.A. Introduction to magnetic helicity. Plasma Phys. Contr. F. 41, B167–B175, 1999.

Chiu, Y.T., Hilton, H.H. Exact Green's function method of solar force-free magnetic-field computations with constant alpha. I. Theory and basic test cases. ApJ 212, 873–885, 1977.

Georgoulis, M.K., LaBonte, B.J. Magnetic energy and helicity budgets in the active region solar corona: I. Linear force free approximation. ApJ, submitted for publication.

Guo, J., Zhang, H., Chumak, O.V., Liu, Y. A quantitative study on magnetic configuration for active regions. Sol. Phys. 237, 25–43, 2006.

Howard, R.F. The magnetic fields of active regions. I. Data and first results. Sol. Phys. 123, 271–284, 1989.

Howard, R.F. The magnetic fields of active regions. VI. Magnetic axis tilt changes. Sol. Phys. 132, 257–270, 1991.

Jing, J., Qiu, J., Lin, J., Qu, M., Xu, Y., Wang, H. Magnetic reconnection rate and flux-rope acceleration of two-ribbon flares. ApJ 620, 1085–1091, 2005.

Liu, Y. Photospheric magnetic field observations during the May 12, 1997 CME and their implications for modeling that event. J. Atmos. Sol.-Terr. Phys. 66, 1283–1293, 2004.

Melrose, D.B. Current paths in the Corona and energy release in solar flares. ApJ 451, 391–401, 1995.

Moffatt, H.K., Ricca, R.L. Helicity and the Clugreanu invariant. Proc. R. Soc. Lond. A 439, 411–429, 1992.

Moon, Y.-J., Choe, G.S., Wang, H., Park, Y.D., Gopalswamy, N., Yang, G., Yashiro, S. A statistical study of two classes of Coronal Mass Ejections. ApJ 581, 694–702, 2002.

Plunkett, S.P., Thompson, B.J., Howard, R.A., Michels, D.J., St. Cyr, O.C., Tappin, S.J., Schwenn, R., Lamy, P.L. LASCO observations of an Earth-directed coronal mass ejection on May 12, 1997. GRL 25, 2477–2480, 1998.

Qiu, J., Yurchyshyn, V.B. Magnetic reconnection flux and Coronal Mass Ejection velocity. ApJ 634, L121–L124, 2005.

Qiu, J., Wang, H., Cheng, C.Z., Gary, D.E. Magnetic reconnection and mass acceleration in flare-Coronal Mass Ejection events. ApJ 604, 900–905, 2004.

Thompson, B.J., Plunkett, S.P., Gurman, J.B., Newmark, J.S., St. Cyr, O.C., Michels, D.J. SOHO/EIT observations of an Earth-directed coronal mass ejection on May 12, 1997. GRL 25, 2465–2468, 1998.

Tian, L., Liu, Y. Tilt and alpha of major flare-producing active regions. A & A 407, L13–L16, 2003.

Webb, D.F., Lepping, R.P., Burlaga, L.F., DeForest, C.E., Larson, D.E., Martin, S.F., Plunkett, S.P., Rust, D.M. The origin and development of the May 1997 magnetic cloud. JGR 105, 27251–27260, 2000.

Yashiro, S., Gopalswamy, N., Michalek, G., St. Cyr, O.C., Plunkett, S.P., Rich, N.B., Howard, R.A. A catalog of white light coronal mass ejections observed by the SOHO spacecraft. JGR 109, Issue A7, CiteID A07105, 2004.

Zhang, J., Dere, K.P., Howard, R.A., Kundu, M.R., White, S.M. On the temporal relationship between Coronal Mass Ejections and flares. ApJ 559, 452–462, 2001.

Zhang, J., Dere, K.P., Howard, R.A., Vourlidas, A. A study of the kinematic evolution of Coronal Mass Ejections. ApJ 604, 420–432, 2004.